ON POSSIBILITY OF RECONSTRUCTING THE REFRACTIVE-INDEX PROFILES OF CIRCULARLY SYMMETRIC CYLINDERS

Kenichi ISHIDA and Mitsuo TATEIBA
Department of Computer Science and Communication Engineering,
Faculty of Engineering, Kyushu University
6-10-1 Hakozaki, Higashi-ku, Fukuoka-shi, Fukuoka 812-81, Japan

1. Introduction

This paper deals with the problem of determining the internal refractive-index of an object from measurement of the scattered wave when a plane wave illuminates the object. Some solutions based on the moment method have been reported for a strongly inhomogeneous object for which the Born approximation is not valid[1–8]. In these solutions, we suffer from the ill-posedness. One approach is to use regularization techniques, but the resolution becomes worse[1, 2]. Another approach is to use optimization techniques in the least-square sense. In this approach, though the equation for optimization is solved without linearization and regularization, the solution may be trapped at a local minimum point and hence the quantitative reconstruction is only possible in a low contrast[5, 6]. Some researchers try to escape the local minima using the simulated annealing approach[7, 8], but it seems that involving parameters should be decided from experiences.

In order to overcome the difficulties, we have used a boundary matching technique for the inverse problem [9–11]. In this technique, the wave is analytically expanded in terms of wave functions, and the mean square error between the measured and calculated scattered-waves is introduced to cast the inverse problem as an optimization problem. In this paper, we investigate the validity of the method and discuss the limit of quantitative reconstruction through computer simulations.

2. Formulation

We review a plane wave scattering by a circularly symmetric dielectric cylinder as shown in Fig.1. The cylinder is divided into N-layers. The radii of each boundary are $r_1, \cdots, r_N$, the refractive indices of each layer are $n_1, \cdots, n_N$, and the refractive index of the surrounding medium is n_0. Here, the permeability is assumed to be the same over all layers. The incident wave u_i is expressed as

$$u_i(\rho, \theta) = \sum_{m=-\infty}^{\infty} i^m J_m(n_0 k\rho) \exp(im\theta), \tag{1}$$

where J_m is the Bessel function of order m, and k is the wavenumber in free space. The scattered wave $\tilde{u}_s$ can be expressed in terms of wave functions as

$$\tilde{u}_s(\rho, \theta, n) = \sum_{m=-\infty}^{\infty} i^m \alpha_m(n) H_m^{(1)}(n_0 k\rho) \exp(im\theta) \qquad (\rho \geq r_1), \tag{2}$$

where $H_m^{(1)}$ is the Hankel function of first kind of order m, α_m is the coefficient to be decided, and n is the refractive-index vector defined as $n = (n_1, \cdots, n_N)$. The total wave Ψ_l $(l = 0, \cdots, N)$ in each layer can be analytically expressed in terms of wave functions as

$$\Psi_l(\rho, \theta) = \sum_{m=-\infty}^{\infty} i^m \{\alpha_{lm} H_m^{(1)}(n_l k\rho) + \beta_{lm} J_m(n_l k\rho)\} \exp(im\theta), \tag{3}$$

where α_{lm} and β_{lm} are the expansion coefficients. The boundary conditions on C_l $(l = 1, \cdots, N)$ are

$$\Psi_{l-1} = \Psi_l, \qquad \frac{\partial \Psi_{l-1}}{\partial \rho} = \frac{\partial \Psi_l}{\partial \rho} \qquad \text{for E-wave case,} \tag{4}$$

$$\Psi_{l-1} = \Psi_l, \qquad \frac{1}{n_{l-1}^2}\frac{\partial \Psi_{l-1}}{\partial \rho} = \frac{1}{n_l^2}\frac{\partial \Psi_l}{\partial \rho} \qquad \text{for H-wave case.} \tag{5}$$

Noting that $\alpha_{Nm} = 0$ and $\beta_{0m} = 1$ for all m, the coefficient α_m can be determined from Eqs.(1)~(5); therefore, the scattered wave can be calculated.

In order to derive the reconstruction algorithm, we introduce the mean square error Ω between the measured and calculated scattered-waves on a circle C including the cylinder as follows:

$$\Omega(\boldsymbol{n}) = \frac{\int_C |u_s(\rho,\theta) - \tilde{u}_s(\rho,\theta,\boldsymbol{n})|^2 ds}{\int_C |u_i|^2 ds} + \frac{\int_C |\partial_\rho u_s(\rho,\theta) - \partial_\rho \tilde{u}_s(\rho,\theta,\boldsymbol{n})|^2 ds}{\int_C |\partial_\rho u_i|^2 ds}, \tag{6}$$

where u_s, $\tilde{u}_s$ and ∂_ρ denote the measured scattered-wave, the scattered wave calculated from Eq.(2) and the derivative in the outward direction normal to C, respectively. The measurement of the scattered wave is carried out on the circle C of radius R. The measured scattered-wave is also expressed in terms of wave functions in the same manner as Eq.(2). The expansion coefficient, which is denoted by γ_m, can be obtained as the Fourier coefficient. Using γ_m, Ω is reduced to the following form without integration.

$$\Omega(\boldsymbol{n}) = \sum_{m=-\infty}^{\infty} |\gamma_m - \alpha_m(\boldsymbol{n})|^2 \left\{ |H_m^{(1)}(n_0 kR)|^2 + 2|H_m^{(1)\prime}(n_0 kR)|^2 \right\}, \tag{7}$$

where $H_m^{(1)\prime}$ denotes the derivative of $H_m^{(1)}$ with respect to the argument.

The inverse problem has resolved itself into the problem of optimizing the vector $\boldsymbol{n}$ for which Ω takes the minimum value. Here, we incorporate a technique of gradually increasing the number of division N into our algorithm to update $\boldsymbol{n}$ stably. The algorithm can be summarized as follows: 1) Assume that the cylinder is homogeneous, i.e., set $N = 1$, and give an initial value to $\boldsymbol{n}$; 2) Update $\boldsymbol{n}$ to decrease Ω; 3) Terminate the process if $\Omega < \varepsilon_1$; 4) If a gradient of $\Omega < \varepsilon_2$, increase the value of N such as $1 \to 2 \to 4$; 5) Go to step 2). Here, ε_1 and ε_2 are convergent criteria, respectively. At step 2), the quasi-Newton method is used for updating $\boldsymbol{n}$, where a finite-difference method is used to estimate a gradient of Ω.

3. Numerical results

Consider the reconstruction of a four-layered cylinder whose outer layer has higher refractive-index. As for the cylinder whose inner layer has higher refractive-index, see [10] for E-wave case and we are now preparing for publishing for H-wave case.

Figures 2 and 3, respectively, show the refractive-index profiles of the lossless cylinder and the lossy cylinder, where n_r and n_i denote the real part and the imaginary part of the refractive-index, respectively. Here, the maximum of n_i, written as $\max(n_i)$, is fixed to 0.0 for lossless case and 0.2 for lossy case. We change the radius and the maximum of n_r, written as $\max(n_r)$, keeping the relation: $r_l = r_1(5-l)/4$, $n_{rl} = 1 + \{\max(n_r) - 1\}(5-l)/4$, $n_{il} = \max(n_i)(5-l)/4$, $(l = 1, \cdots, 4)$. In the simulation, the initial value of the refractive-index vector $\boldsymbol{n}$ is set to that in free space, i.e., $1.0 + i0.0$. The maximum value of $|m|$ in Eq.(7) is set to M, which is the minimum number to satisfy $|H_M(n_0 kR)\gamma_M|^2 < 10^{-13}$, and $R = 2r_1$, $\varepsilon_1 = \varepsilon_2 = 10^{-7}$ are used. The measured-scattered wave is assumed to be noise-free. To estimate the error of reconstructed profile, we introduce the profile error defined by $Err = \sqrt{\sum_{l=1}^{N} |\tilde{n}_l - n_l|^2} \Big/ \sqrt{\sum_{l=1}^{N} |n_l|^2}$, where $\tilde{n}_l$ and n_l are the reconstructed and original refractive-indices of layer l, respectively.

Figures 4 and 5 show the profile errors for lossless cylinders at the final stage for E-wave case and H-wave case, respectively, where λ is the wavelength in free space. For cylinders

corresponding to sunken points, the algorithm works well and the accurate reconstructed profiles are obtained. Roughly speaking, we can see that the accurate profiles are obtained by the algorithm for lossless cylinders such as $\{\max(n_r)-1\}r_1/\lambda < 0.3$ for E-wave case, and $\{\max(n_r)-1\}r_1/\lambda < 0.4$ for H-wave case, respectively. Outside of the above limits, $\Omega(n)$ has local minimum points on the way from the initial point to the minimum point; hence, the solution may be trapped at a local minimum point. These show the limits of quantitative reconstruction for strong inhomogeneity. For small cylinders such as $r_1/\lambda < 0.5$, the profile errors are also large. For these cylinders, since Ω is minimized up to good extent, this result suggests the limit of resolution by the algorithm.

Figures 6 and 7 show the profile errors for lossy cylinders at the final stage. Accurate profiles are obtained for cylinders which have higher refractive-indices, and the above limits for strong inhomogeneity are released. Many simulations show that local minimum points appear when the imaginary part of n is close to zero. Therefore, the optimizing process may hardly come across the local minimum points for lossy cylinders.

We reconstructed the cylinders also from the measured scattered-wave in a noisy situation. In this case, the profile errors become larger for lossy cylinders than that for lossless cylinders. The reason may be that the waves through lossy cylinders are decayed and sensitive to noise.

Compared with the cylinders whose inner layers have higher refractive-indices, it seems that the range within which the algorithm is valid is restricted. But, the average refractive-index over all layers is actually higher for the cylinders whose outer layers have higher refractive-indices since the cross section of outer layers is larger. Considering this fact, we conclude that the applicability limit of our algorithm depends mainly on the average refractive-index in the rate of space occupation and does not change largely with the refractive index of each layer in the cylinder if the average is constant.

4. Conclusion

The probability of reconstructing the profile of a dielectric cylinder whose outer layer has higher refractive-index in free space using a boundary matching technique has been shown by computer simulations. For lossless cylinders, the range within which the accurate profiles are obtained seems a little wider for H-wave case than that for the E-wave case. For lossy cylinders, the accurate profiles are obtained for stronger inhomogeneity. These results agree with the results for the cylinders whose inner layers have higher refractive-indices. Although considering a circular symmetric cylinder in this paper, we guess that the limit of reconstruction presented here may not be overcome by other methods under the same conditions also for a cylinder whose shape is non-circular and whose profile is asymmetric.

References

[1] N. Joachimowicz, C. Pichot, and J.-P. Hugonin, IEEE Trans. Antennas & Propag., 39, 12, 1742–1752, 1991.

[2] S. Caorsi, G. L. Gragnani, and M. Pastorino, IEE Proc.-H, 139, 1, 45–52, 1992.

[3] W. Wang and S. Zhang, IEEE Trans. Antennas & Propag., 40, 11, 1292–1296, 1992.

[4] C.-C. Chiu and R.-H. Yang, Micro. Opt. Tech. Lett., 9, 5, 292–302, 1995.

[5] R. E. Kleinman and P. M. van den Berg, J. Comp. Appl. Math., 42, 17–35, 1992.

[6] H. Harada et al., IEEE Trans. Antennas & Propag., 43, 8, 784–792, 1995.

[7] S. Caorsi et al., Radio Sci., 30, 1, 291–301, 1995.

[8] J. W. Ra and C. S. Park, Proc. URSI Int. Symp. on EM Theory, 261–263, 1995.

[9] K. Ishida, T. Kudou, and M. Tateiba, IEICE Trans. Electron., E77-C, 11, 1837–1840, 1994.

[10] K. Ishida, T. Kudou, and M. Tateiba, In JSAEM Studies in Applied Electromagnetics vol.4, JSAEM, (to be published in 1996)

[11] T. Kudou, K. Ishida, and M. Tateiba, In JSAEM Studies in Applied Electromagnetics vol.4, JSAEM, (to be published in 1996)

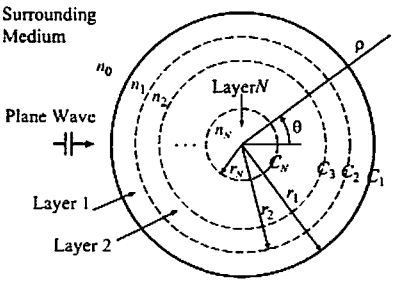

Figure 1: A circularly symmetric dielectric cylinder

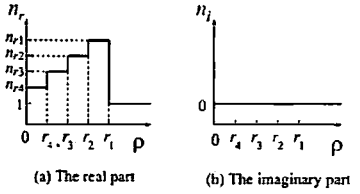

Figure 2: Refractive-index profile of a four-layered lossless cylinder.

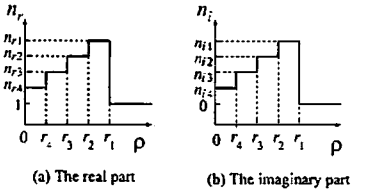

Figure 3: Refractive-index profile of a four-layered lossy cylinder.

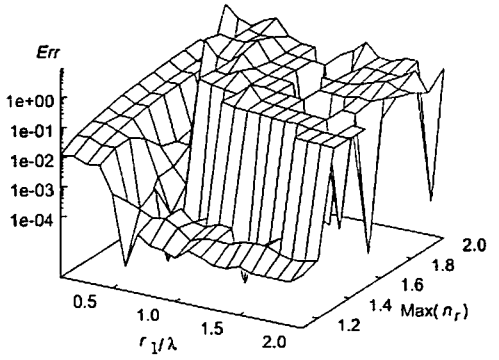

Figure 4: The profile errors for lossless cylinders in E-wave case

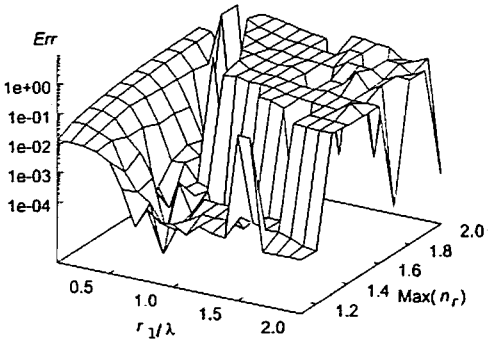

Figure 5: The profile errors for lossless cylinders in H-wave case

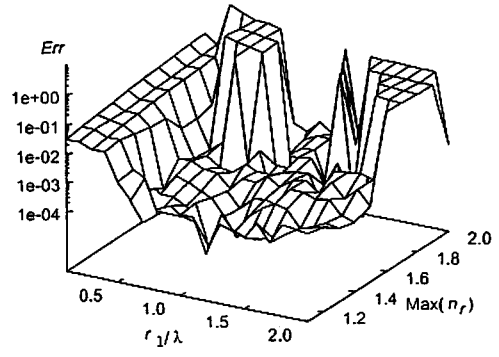

Figure 6: The profile errors for lossy cylinders in E-wave case

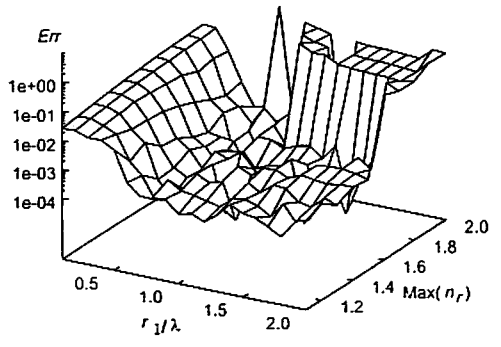

Figure 7: The profile errors for lossy cylinders in H-wave case